Materials Science

AIMS Materials Science, 6(1): 10–24.
DOI: 10.3934/matersci.2019.1.10
Received: 16 October 2018
Accepted: 09 December 2018
Published: 02 January 2019

http://www.aimspress.com/journal/Materials

Research article

Water-repellent glass coated with SiO_2–TiO_2–methyltrimethoxysilane through sol–gel coating

Alfa Akustia Widati[1,2,]*, Nuryono Nuryono[1,]* and Indriana Kartini[1]

[1] Department of Chemistry, Faculty of Mathematics and Natural Sciences, Universitas Gadjah Mada, Sekip Utara, Yogyakarta 55281, Indonesia
[2] Departement of Chemistry, Faculty of Science and Technology, Universitas Airlangga, Surabaya 60115, Indonesia

* **Correspondence:** Email: nuryono_mipa@ugm.ac.id, alfaakustia@fst.unair.ac.id.

Abstract: A hydrophobic coating for glass substrates was developed using SiO_2, TiO_2, and methyltrimethoxysilane (MTMS) to achieve low surface energy and a rough surface. The coating process was conducted using a sol–gel method and layer by layer deposition. The effect of SiO_2, TiO_2, and MTMS on the hydrophobicity and transparency of the coating were evaluated using contact angle and optical transmittance measurements, respectively. The transparency was found to decrease with higher moles of SiO_2, TiO_2, and MTMS; the water contact angle initially increased with increasing addition of these reagents, but then declined above the optimum conditions. The optimum conditions were determined to be at approximately 0.075, 0.030, and 0.002 mol of SiO_2, TiO_2, and MTMS, respectively. The resulting water contact angle was $115.56 \pm 1.01°$. SiO_2 and TiO_2 provided a synergistic effect to improve the roughness surface, as shown in the AFM data. The glass coated using SiO_2–TiO_2–MTMS exhibited higher hardness values than bare glass.

Keywords: hydrophobic glass; SiO_2; TiO_2; methyltrimethoxysilane; rough surface

1. Introduction

Hydrophobic glasses are glasses with surfaces that exhibit water roll-off properties. Generally, the hydrophobicity of a glass is influenced by its surface energy and surface roughness [1]. Fluorosilane is the most frequently used low-surface-energy material. Unfortunately, fluorosilane is categorized as a toxic compound, and has been reported to be hazardous to human health and environment [2,3]. Recently, many authors have utilized alkylsilane as a milder alternative to fluorosilane that also has a low surface energy [4–7]. However, materials coated with alkylsilane exhibited lower water contact angles than those coated with fluorosilane. Coatings prepared using only alkylsilane also resulted in low water contact angles, i.e., low hydrophobicity. The coating of glasses with methyltrimethoxysilane (MTMS) also resulted in a low water contact angle; however, the angle was increased to 171 ± 1° by the addition of polymethylmethacrylate to the MTMS coating [8]. Another attempt to improve the hydrophobicity of a silica aerogel based on MTMS through modification with trimethylchlorosilane (TMCS) and cetyltrimethylammoniumbromide was reported [9].

Increasing the roughness of a surface can also enhance its hydrophobicity. This effect can be explained by the Wenzel and Cassie-Baxter equation. Wenzel stated that a rough surface has an actual surface area larger than its horizontal projection. The substitution of the actual surface area to the Young equation will provide the larger contact angle. Cassie-Baxter assumed that the rough surface is created by air entrapment in the gaps of the rough structure, so that the droplet rests on a layer of air [10,11]. A rough surface can be produced by the deposition of metal oxide on the surface. The agglomeration of the oxide generates some cavities on the surface, producing a rough structure. In previous studies, we have investigated the use of SiO_2 nanoparticles, methyltrimethoxysilane, and hexadecyltrimethoxysilane to prepare hydrophobic glasses [12]. The prepared glasses were stable towards ethanol, but unstable at ambient temperature. The use of SiO_2 nanoparticles in powder form decreased the transparency of the glasses. The use of a MTMS-modified SiO_2 sol to coat soda lime glass resulted in high transparency, but its water contact angle was less than 90° [13].

In addition to SiO_2, TiO_2 has also been employed to produce rough surfaces [14–16]. Interestingly, the combination of TiO_2 and hydrophobic agents results in tunable properties, i.e., the ability to switch the hydrophobicity to hydrophilicity under UV illumination [17,18]. The aquapel modified micro-nano TiO_2/SiO_2 composite films had reversible high-hydrophobic to high-hydrophilic conversion properties [17]. Crystalline TiO_2 plays a main role in this behavior. The irradiation of TiO_2 is known to produce electrons and holes. The electrons tend to reduce Ti^{4+} to the Ti^{3+}, and the holes oxidize the O^{2-} on the surface. Oxygen atoms are ejected, generating oxygen vacancies. At this stage, water molecules occupy these vacancies, resulting in adsorbed hydroxyl groups. This behavior created the hydrophilic properties [19]. In other words, to obtain stable hydrophobicity using modified TiO_2, the TiO_2 structure must be amorphous [20]. The amorphous TiO_2 has a much a higher band gap (~310 nm) than crystalline TiO_2 (~400 nm), therefore it is promising candidate to performance the UV-shielding ability [21]. The coating of TiO_2 with inert material such as SiO_2 also inhibits the photocatalytic properties of TiO_2. Hybrid SiO_2–amorphous TiO_2 also exhibited excellent stability under UV-light irradiation. SiO_2 imparts an efficient UV scattering because of the large refractive index of SiO_2 [22].

The mechanical properties of coatings are an important aspect from an applications point of view. Generally, hydrophobic coatings have low mechanical stability due their high surface roughness. Liu et al. [23] reported the poor scratch resistance of such coatings; the coatings were easy removed using all pencil hardnes (hardest, average hardness, and softest pencil). TiO_2 and SiO_2 have been introduced into hybrid silica–epoxy coatings to improve the mechanical properties of an aluminum alloy surface. The addition of TiO_2 improved the hydrophobic and adhesion properties of the coating. However, it decreased the hardness of the coated surfaces. Meanwhile, SiO_2 increased the hydrophobicity and surface hardness, but the coatings exhibited poor adhesion properties [24].

In this work, we proposed the fabrication of hydrophobic glass using MTMS-modified SiO_2–TiO_2. MTMS contributed to the increased hydrophobicity due to replacement of the polar –OH groups of the surface by the non-polar $–CH_3$ groups of MTMS. SiO_2 and TiO_2 produced a rough surface and contributed to the hardness of coating. The effect of chemical composition on water contact angle and transparency of the coated glasses was studied. The topography of the surface, the hardness properties and the stability of the hydrophobic glass were also determined.

2. Materials and method

2.1. Materials

The sol–gel system consisted tetraethylorthosilicate (TEOS) and titanium tetraisopropoxide (TTIP) as SiO_2 and TiO_2 precursor, methyltrimethoxysilane (MTMS) as the hydrophobic precursor, HCl as catalyst, and ethanol as solvents. All these chemicals were purchased from Sigma Aldrich, except TEOS was supplied by Merck. All reagents were commercially available in analytical grade. All these materials were used as received without any further purification.

2.2. Coating preparation

Before the coating process, glass slides were sonicated in ethanol bath for 30 minutes and were dried. The coating solutions were prepared by the sol–gel method. SiO_2, TiO_2, and MTMS sol were hydrolyzed in separate containers. A 0.030 mol of SiO_2 was prepared by stirring a solution consisting 3.35 mL of TEOS, 8 mL of ethanol, 1 mL of water, and 0.2 mL of 0.1 M HCl at 60 ℃ for 90 minutes. After this, the obtained SiO_2 sol was added 2 mL of concentrated HCl, followed by adding ethanol to a 20 mL of solution. To clarify the effect of SiO_2 on the hydrophobization, various mol SiO_2 (0, 0.015, 0.030, 0.045, 0.060, 0.075 and 0.089) were employed.

The procedure for preparation of TiO_2 and MTMS sol were similar with early described procedure in the preparation of SiO_2 sol. The variation mol of TiO_2 (0, 0.015, 0.030 and 0.045) and MTMS (0, 0.001, 0.002, 0.004 and 0.006) were also prepared to study the effect on the hydrophobization. While the mol of SiO_2 was varied, we kept constant the mol of TiO_2 and MTMS were 0.030 and 0.002 mole, respectively. Furthermore, the optimum mol of SiO_2 and constant mol of MTMS was handled to study the effect of TiO_2 amount. After that, the variation of MTMS mol was investigated using optimum mol of SiO_2 and TiO_2.

The deposition of SiO_2, TiO_2, and MTMS on glass substrates were conducted by layer by layer dip coating technique. The bottom, middle, and top layer were SiO_2, TiO_2, and MTMS, respectively. The glasses were immersed into the coating solution with withdrawal speed of 3 cm/min. After each coating, the films were first annealed at room temperature (33 ℃) for 10 minutes and then followed at 70 °for 30 minutes.

2.3. Characterization

Shimadzu UV 1800 was used to determine the transparency of coated glass. The transmissions were measured in the wavelength range 300–800 nm. Vickers microhardness Mitutoyo HM 211 was employed to measure the mechanical durability. The average of five hardness test was found for each of coated glass. FTIR spectra was recorded on Shimadzu IRTracer-100. Spectrum was recorded in the wavenumber range 4000–400 cm^{-1}. The structure of sample performed on the XRD Pan Analytical using Cu Kα radiation of wavelength 0.15418 nm. The diffraction data were recorded between 5–100 ° with 2 minutes scan speed. The surface roughness of coated glass was observed AFM N8 Neos Bruker in the non-contact mode under ambient conditions. Water contact angles were determined by capturing the images of a 40 μL water droplet on coated glasses. The images were then processed using ImageJ software. The morphology and composition of surface was analyzed using SEM-EDX Carl Zeiss EVO MA 10.

3. Results and discussion

The coating solutions were formed by the hydrolysis and condensation reactions of MTMS, TEOS, and TTIP. The sol–gel process of TEOS, TTIP, and MTMS was conducted using ethanol, water, and HCl. Hydrolysis occurred when TEOS was dissolved in a water–ethanol mixture. This process resulted in the formation of silanol (Si–OH) groups. The condensation of the silanol groups formed siloxane bridges (–Si–O–Si–), while the hydrolysis of TTIP produced the tetravalent cation titanol, ($Ti(OH)_4$). Oxolation and olation processes also occurred during nucleation and growth, generating amorphous TiO_2 [25]. In this research, of amorphous TiO_2 was prepared to reduce the photocatalytic properties of TiO_2 in order to maintain the hydrophobic properties of the coated glasses.

Simultaneously, MTMS was polymerized in a water–ethanol mixture under acidic conditions. Water was an important solvent in the hydrolysis process of MTMS. Although the process is catalyzed by HCl, the methoxy groups of MTMS cannot completely hydrolyze unless water is present in the sol–gel system [9]. The three methoxy groups of the MTMS monomers underwent hydrolysis and condensation reactions, and the monomers condensed to form dimers. After 1 hour, condensation of the dimers resulted in tetramers, which then transformed into a 4-membered ring [26].

The coating process was conducted by immersing the glass substrate into each of the sols, followed by annealing at 70 ℃. During the annealing process, the hydroxyl groups condensed, forming Si–O–Si and Si–O–Ti networks.

3.1. XRD analysis

In order to investigate the phases of SiO_2, TiO_2, MTMS and SiO_2–TiO_2–MTMS, the sol was heated at 70 ℃, ground into a powder, and then used in XRD and FTIR analysis. This temperature was similar to the annealing temperature of the coated glass. Heating the sol at 70 ℃ did not change the crystallinity of the sample, so we used this temperature to prepare the powder form of the samples. The corresponding XRD spectra of the samples are depicted in Figure 1.

The XRD patterns reveal that none of the samples exhibited sharp peaks. In the diffractogram of SiO_2, the hump at 2θ 15–35 ° indicates that the sample was amorphous silica. The XRD pattern of TiO_2 also indicated that our sample had an amorphous structure. The amorphous structure of TiO_2 was important to obtain the hydrophobic properties in our coated glasses, because amorphous TiO_2 does not exhibit the strong photocatalytic properties associated with crystalline TiO_2 [20]. As discussed earlier, photocatalysis produces hydrophilic OH groups. Hence, crystalline TiO_2 is not a suitable structure to prepare hydrophobic materials. The MTMS pattern displayed a diffraction peak at 10 ° and a broad peak at 14–30 °. The first peak was related to the presence of silicon atoms attached to alkyl groups, while the second peak was associated with Si–O–Si in amorphous silica [27]. Therefore, it was not surprising that the diffractogram of SiO_2–TiO_2–MTMS showed the amorphous phase.

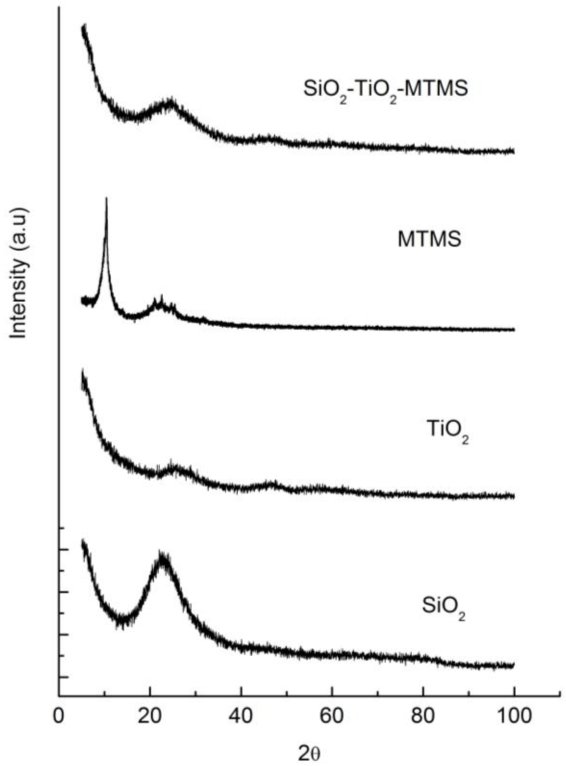

Figure 1. Diffractograms of prepared SiO_2, TiO_2, MTMS, and SiO_2–TiO_2–MTMS samples.

3.2. FTIR spectra

The FTIR spectra of SiO_2, TiO_2, MTMS, and SiO_2–TiO_2–MTMS are shown in Figure 2. The details of the SiO_2, TiO_2, MTMS, and SiO_2–TiO_2–MTMS spectra are presented in Table 1. FTIR analysis was conducted to study the appearance of the SiO_2, TiO_2, and MTMS peaks in the SiO_2–TiO_2–MTMS sample.

All the spectra displayed a broad band in the spectral region 3200–3500 cm^{-1}, which was related to O–H stretching from silanol, titanol, absorbed water, and ethanol. The peak at 1620–1630 cm^{-1} corresponds to the O–H vibration of H_2O. The spectra of SiO_2–TiO_2–MTMS showed characteristic peaks at 1438, 1271, 1120, 931, and 775 cm^{-1}. The peak at 1438 cm^{-1} was assigned to antisymmetric bending of the C–H bond of the CH_3 of MTMS. The peak at 1271 cm^{-1} was the symmetric bending of the C–H bond in CH_3 from MTMS. The peak at 1120 cm^{-1} corresponded to overlapping peaks of the antisymmetric stretching of Si–O–C and symmetric stretching of Si–O–Si in cyclic structures. The antisymmetric stretching of Si–O–C originated from the MTMS molecules. Meanwhile, the symmetric stretching of Si–O–Si in cyclic structures was attributed to the polymerization of SiO_2 and MTMS, respectively. The peak at 931 cm^{-1} was related to non-bridging Si–O that had broken free from SiO_2 and MTMS. Evidence for Si–O–Ti linkages between SiO_2 and TiO_2 was also obtained from this peak, i.e., in the range between 900–960 cm^{-1} [28]. The peak at about 775 cm^{-1} indicated the C–H stretch of MTMS. The peak at 630 cm^{-1} was confirmed to be the Ti–O–Ti vibration of TiO_2.

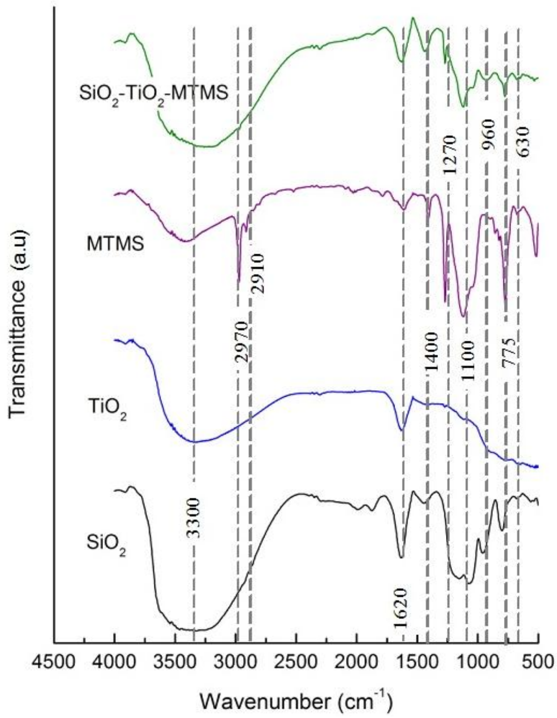

Figure 2. FTIR spectra of the powders obtained from the SiO_2, TiO_2, and MTMS sols and SiO_2–TiO_2–MTMS coated glass.

Table 1. Characteristic infrared absorption of SiO_2, TiO_2, and SiO_2–TiO_2–MTMS.

Wavenumber (cm^{-1})	Sample				Assignment
	SiO_2	TiO_2	MTMS	SiO_2–TiO_2–MTMS	
3200–3500	√	√	√	√	O–H stretching [28,29]
2970			√		Antisymmetric stretching C–H bond in CH_3 [30]
2910			√		Symmetric stretching C–H bond [3]
1620–1630	√	√	√	√	O–H vibration of H_2O [31]
1400–1440			√	√	Antisymmetric bending C–H bond in CH_3 [30]
1270			√	√	Symmetric bending C–H bond in CH_3 [31]
1070–1160	√		√	√	Antisymmetric stretching of Si–O–C Symmetric stretching of Si–O–Si in cyclic structures [28]
930–960	√			√	Si–O non bridging free broken [27] Vibration of Si–O–Ti [28]
773–775			√	√	Stretching of C–H [32,33]
630		√		√	Ti–O–Ti vibration [34,35]

3.3. Wettability behavior of the glass coatings

The wettability of the coated glass was studied using various moles of the coating solutions. The changes in the contact angles and shapes of water droplets for different amount of SiO_2, TiO_2, and MTMS are shown in Figures 3 and 4. Figure 3a depicts the effect of the mol of SiO_2 and TiO_2 on the contact angle of the glass substrates. The water contact angle on the coated glasses increased when the mol of SiO_2 was raised, reaching 110.14 ± 1.01 ° at 0.075 mol SiO_2. This increase in water contact angle may be attributed to the increase in surface roughness from the network formation of silica particles.

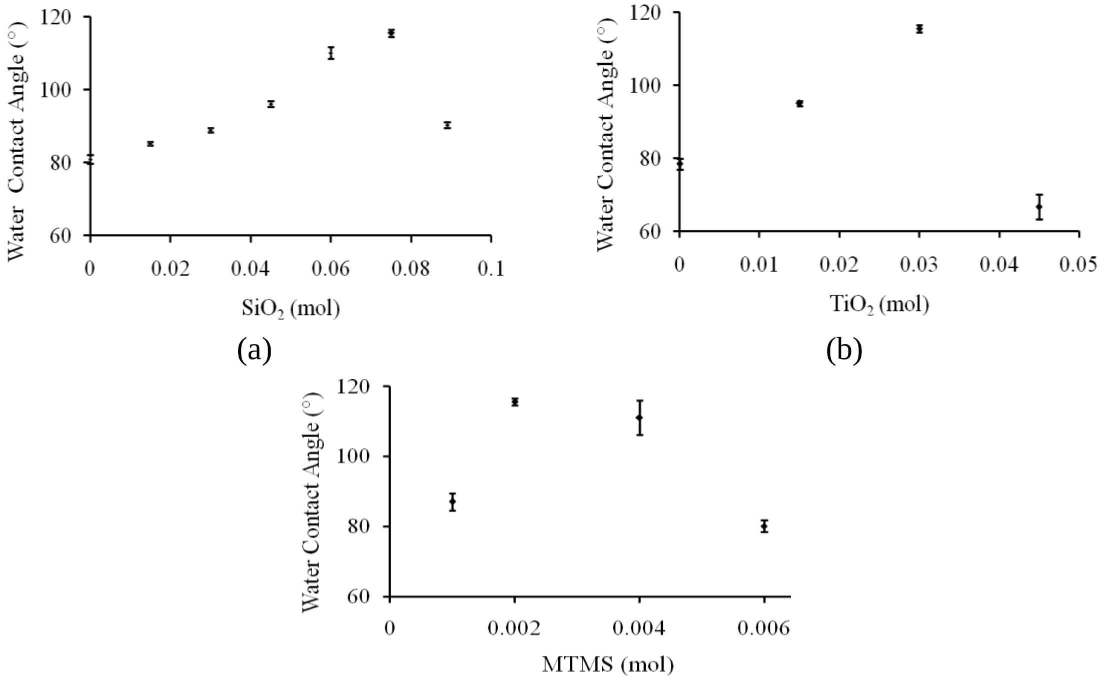

Figure 3. The effect of the mol of (a) SiO_2, (b) TiO_2, (c) MTMS on the hydrophobicity of glass coated with SiO_2–TiO_2–MTMS through layer by layer deposition.

In contrast, the contact angle decreased to 90.34 ± 0.85 ° when 0.089 mol SiO_2 was used in the glass coatings. The abundance of hydroxyl groups on the surface caused an increase in its hydrophilicity. This tendency can be attributed to higher interaction of polar hydroxyl group with water molecule [36]. It was also assumed that the roughness tend to be smooth because the homogeneity of SiO_2 coating on glass surfaces.

The influence of the mol of TiO_2 on hydrophobicity and transparency can be seen in Figure 3b. Coating glasses with sols containing 0 to 0.030 mol of TiO_2 caused increased hydrophobicity. This result was unsurprising, as TiO_2, like SiO_2, is used to enhance the surface roughness; therefore the effect of TiO_2 was similar to that of SiO_2. Based on the results, 0.075 mol of SiO_2 and 0.030 mol of TiO_2 were used in further studies.

Figure 3c shows the contact angles when different amount of MTMS were used in the glass coating. The hydrophobicity decreased with increasing amounts of MTMS, reaching 115.56 ± 1.01 °

when 0.002 mol of MTMS was used. This might be due to the replacement the polar OH groups by the non-polar alkyl groups of MTMS which has low surface energy. Furthermore, the water contact angle decreased when more than 0.002 mol of MTMS was used. In high concentration of silane, the surface did not show any hierarchical morphology. The surfaces with rather smooth with holes, therefore the water contact angle were decreased [37].

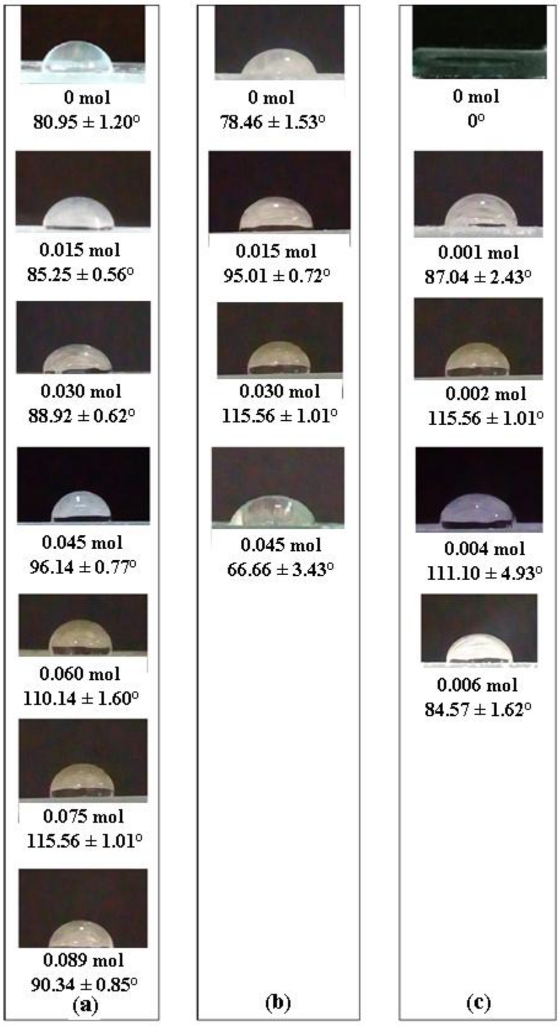

Figure 4. The droplet images of SiO_2–TiO_2–MTMS coated glasses for various moles of (a) SiO_2, (b) TiO_2 and (c) MTMS.

3.4. Optical studies of coated glasses

Figure 5 shows the optical transmission of the coated glasses prepared using various moles of SiO_2, TiO_2, and MTMS. The transparency of the bare glass decreased when the coating solution was deposited on the surface. Increasing the mol of SiO_2, TiO_2, or MTMS in the coating solution resulted in decreased transparency of the coated glass. Higher moles of these components in the coating solutions promoted the formation of thicker films. A previous study also reported that the preparation of transparent glass with high surface roughness was difficult, because the higher-roughness coatings were thicker and led to extensive light scattering and loss of transparency [38].

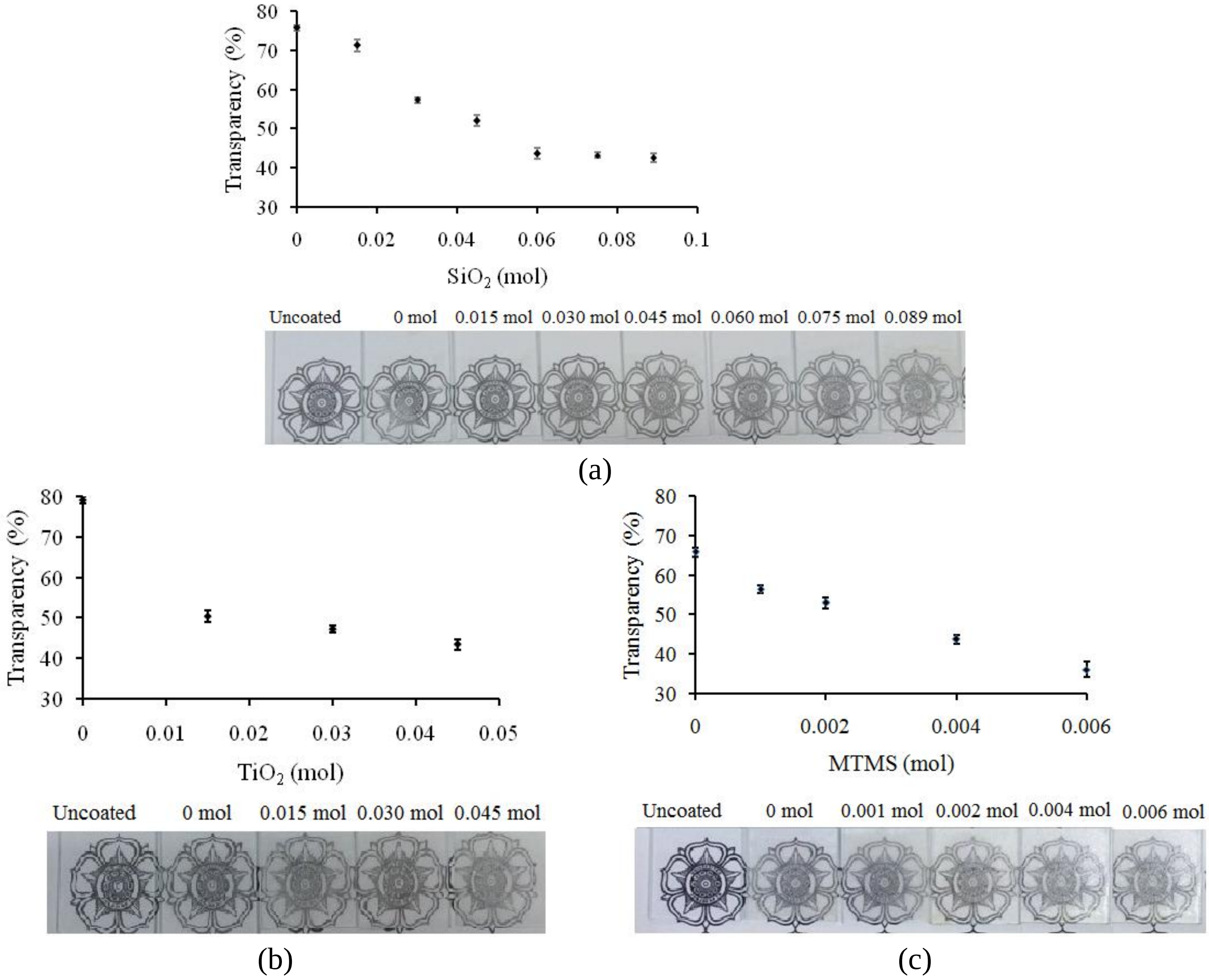

Figure 5. Transparency and optical photographs of coated glass samples for various mol of (a) SiO_2, (b) TiO_2 and (c) MTMS.

3.5. Surface morphology and roughness studies

SiO_2 and TiO_2 played a crucial role in the wettability of the surfaces. The water contact angle measured for the SiO_2–MTMS coated glass was 78.46 ± 1.53°. The contact angle increased when TiO_2 was deposited on the surface. The SiO_2–TiO_2–MTMS coated glass exhibited a water contact angle about 115.56 ± 1.01°, because the use of a combination of SiO_2 and TiO_2 in the coating produced a rougher surface than when only SiO_2 was used. This was confirmed by the AFM analysis results, as can be seen in Figure 6. The surface topography revealed that the rms of bare glass, and of glass coated using SiO_2–MTMS, TiO_2–MTMS, and SiO_2–TiO_2–MTMS were 4.10, 95.6, 76.3, and 106.0 nm, respectively.

Table 2 tabulated the height surface of coated glass based on two-dimensions of AFM images. It can be seen that the surface height of SiO_2–MTMS, TiO_2–MTMS, and SiO_2–TiO_2–MTMS were 70–200, 10–90, and 20–180 nm, respectively. This data showed that the surface height of SiO_2–TiO_2–MTMS was resulted from a combination of height surface between SiO_2–MTMS and TiO_2–MTMS. The topography and high surface roughness of SiO_2–TiO_2–MTMS was resulted from the aggregation of SiO_2 and TiO_2 particles. In other word, SiO_2 and TiO_2 had a constructive effect on the surface roughness.

SiO_2–TiO_2–MTMS performed rougher surface, higher water repellence, and Cassie-Baxter behavior. In the Cassie-Baxter model, air is trapped in the cavities, and the water droplets rest on top of the rough surfaces. The results of the SEM-EDX measurements also demonstrated that the SiO_2–TiO_2–MTMS coated glass had a rough surface with a coating thickness about 18 μm. This information is presented in Figure S1 of the supplementary material.

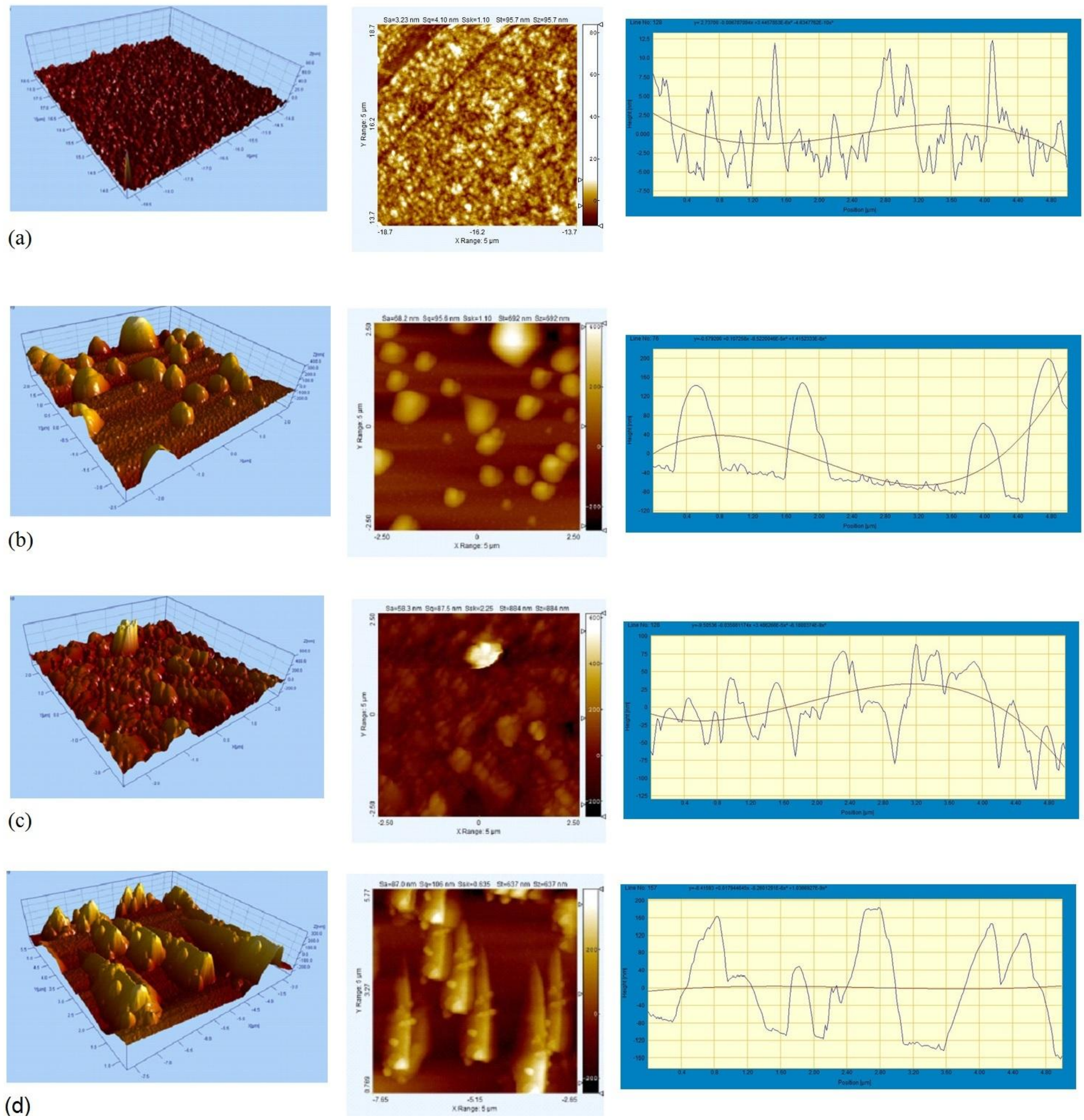

Figure 6. AFM comparison of the surface roughness of (a) uncoated glass, and glass coated with (b) SiO_2–MTMS (c) TiO_2–MTMS, and (d) SiO_2–TiO_2–MTMS.

Table 2. The roughness parameter of coated and uncoated glass by AFM measurements.

Sample	Height of surface (nm)	rms (nm)
Bare glass	0.5–12	4.10
SiO_2–MTMS	70–200	95.6
TiO_2–MTMS	10–190	76.3
SiO_2–TiO_2–MTMS	20–180	106.0

The surface roughness also influenced the transparency of glasses. The ability of glass to transmit light waves is called transparency. Rough surfaces have tendency to absorb and transmit the light. Therefore, the transmission process on the rough surface was lower than smooth surfaces. It caused the rough surfaces presented low transparency. Figure 7 displays the correlation between surface roughness and transparency.

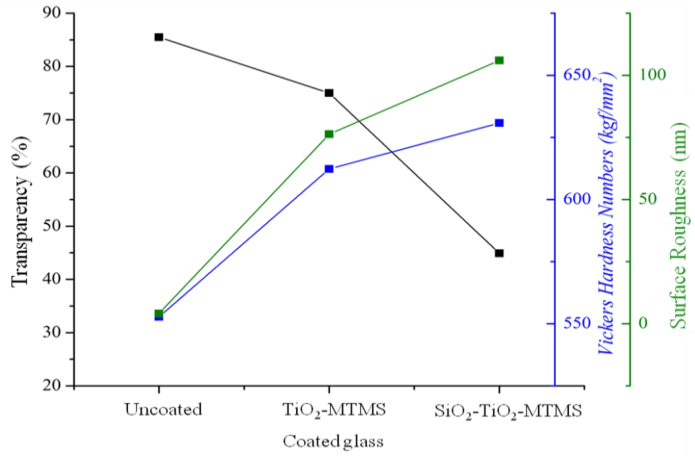

Figure 7. Transparency in relation to hardness properties and surface roughness of coated glasses.

3.6. Mechanical properties determined by the Vickers hardness

The mechanical properties of the hydrophobic glasses were evaluated using the Vickers hardness test, which measures the hardness as a function of the penetration depth of an indentor. The thicker the coating is, the deeper the penetration of the indentor, and the higher the hardness is considered to be [39]. The hardness properties of bare glass and glass coated with TiO_2–MTMS and SiO_2–TiO_2–MTMS were 552.76, 612.32, and 615.1 kgf/mm^2, respectively. The higher value for coated glass than bare glass might due to its higher thickness. Lakshmi et al. reported that the formation of a siloxane network enhanced the thickness of a coating [38]. Increasing the hardness of coated glasses decreased their transparency, as shown in Figure 7.

3.7. Stability of the coatings

The stability of coatings is a very important property from an applications point of view. Here, we measured the changes in the water contact angle as a function the long-term outdoor exposure time, as shown in Figure 8. The water contact angle decreased slightly to 89.37° after 4 weeks. One reason for this behavior was the accumulation of dirt. The presence of the silica coating on the surface produced hydroxyl groups, and also adsorbed moisture from the atmosphere, decreasing the water contact angle [8]. Li et al. also reported that coatings fabricated using the sol–gel technique exhibited poor moisture resistance because the existence of hydroxyl groups [40].

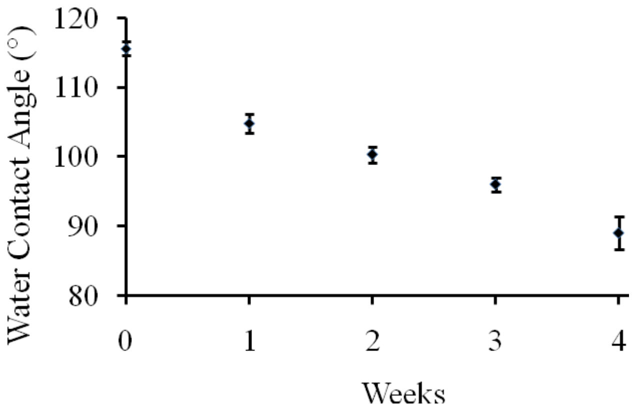

Figure 8. The outdoor stability of glass coated with 0.075 mol of SiO_2, 0.030 mol of TiO_2, and 0.002 mol of MTMS.

4. Conclusions

Hydrophobic glasses were successfully synthesized from SiO_2, TiO_2, and MTMS precursors. The addition of TiO_2 to SiO_2–methyltrimethoxysilane coated glass increased the surface roughness and improved the hydrophobicity. Higher moles of SiO_2, TiO_2, and MTMS produced higher hydrophobicity, but lowered the transparency of the coated glasses. The hydrophobic glasses exhibited good hardness. A coating with 0.075 mol of SiO_2, 0.030 mol of TiO_2, and 0.002 mol of MTMS was found to have high hydrophobicity, rough surface and good mechanical properties. Further research into maintaining high transparency in the glasses through controlling the surface roughness can be proposed.

Acknowledgments

The authors are grateful for financial support from Ministry or Research, Technology and Higher Education, Indonesia through PDD Grant of Universitas Airlangga No. 122/SP2H/PTNBH/DRPM/2018. We also thank to the Department of Chemistry, Faculty of Mathematics and Natural Sciences, Universitas Gadjah Mada and Department of Chemistry, Faculty of Science and Technology, Universitas Airlangga for the use of laboratory facilities.

Conflicts of interest

There is no conflict to declare.

References

1. Song J, Rojas OJ (2013) Approaching super-hydrophobicity from cellulosic materials: A review. *Nord Pulp Pap Res J* 28: 216–238.
2. Nørgaard AW, Hansen JS, Sørli JB, et al. (2013) Pulmonary toxicity of perfluorinated silane-based nanofilm spray products: solvent dependency. *Toxicol Sci* 137: 179–188.
3. Pan G, Zhou Q, Luan X, et al. (2014) Distribution of perfluorinated compounds in Lake Taihu (China): Impact to human health and water standards. *Sci Total Environ* 487: 778–784.
4. Wang H, Ding J, Lin T, et al. (2010) Super water repellent fabrics produced by silica nanoparticle-containing coating. *Res J Text Apparel* 14: 30–37.
5. Rostamzadeh P, Mirabedini SM, Esfandeh M (2014) APS-silane modification of silica nanoparticles effect of treatment's variables on the grafting content and colloidal stability of the nanoparticles. *J Coat Technol Res* 11: 651–660.
6. Spataru CI, Purcar V, Donescu D, et al. (2013) Preparation of hydrophobic surface based on hybrid silica films by sol–gel process. *UPB Sci Bull B* 75: 117.
7. Wang X, Chai Y, Liu J (2013) Formation of highly hydrophobic wood surfaces using silica nanoparticles modified with long-chain alkylsilane. *Holzforschung* 67: 667–672.
8. Kavale MS, Mahadik DB, Parale VG, et al. (2011) Optically transparent, superhydrophobic methyltrimethoxysilane based silica coatings without silylating reagent. *Appl Surf Sci* 258: 158–162.
9. He S, Chen X (2017) Flexible silica aerogel based on methyltrimethoxysilane with improved mechanical property. *J Non-Cryst Solids* 463: 6–11.
10. Mohamed AM, Abdullah AM, Younan NA (2015) Corrosion behaviour of superhydrophobic surfaces: A review. *Arab J Chem* 8: 749–765.
11. Brassard JD, Sarkar DK, Perron J (2012) Fluorine based superhydrophobic coatings. *Appl Sci* 2: 453–464.
12. Widati AA, Nuryono N, Kartini I, et al. (2017) Silica-methyltrimethoxysilane based hydrophobic coatings on glass substrate. *J Chem Technol Metall* 52: 1123–1128.
13. Philipavičius J, Kazadojev I, Beganskienė A, et al. (2008) Hydrophobic antireflective silica coatings via sol–gel process. *Mater Sci* 14: 283–287.
14. Paz Y (2011) Self-assembled monolayers and titanium dioxide: From surface patterning to potential applications. *Beilstein J Nanotech* 2: 845–861.
15. Kartini I, Santosa SJ, Febriyanti E, et al. (2014) Hybrid assembly of nanosol titania and dodecylamine for superhydrophobic self-cleaning glass. *J Nanopart Res* 16: 2514.
16. Shi YL, Feng XJ, Yang W, et al. (2011) Preparation of super-hydrophobic titanium oxide film by sol–gel on substrate of common filter paper. *J Sol-Gel Sci Techn* 59: 43–47.
17. Li W, Guo T, Meng T, et al. (2013) Enhanced reversible wettability conversion of micro-nano hierarchical TiO_2/SiO_2 composite films under UV irradiation. *Appl Surf Sci* 283: 12–18.
18. Liu K, Cao M, Fujishima A, et al. (2014) Bio-inspired titanium dioxide materials with special wettability and their applications. *Chem Rev* 114: 10044–10094.
19. Wu KR, Wang JJ, Liu WC, et al. (2006) Deposition of graded TiO_2 films featured both hydrophobic and photo-induced hydrophilic properties. *Appl Surf Sci* 252: 5829–5838.

20. Huang J, Lin Y, Lu L, et al. (2012) The photocatalytic properties of amorphous TiO_2 composite films deposited by magnetron sputtering. *Res Chem Intermediat* 38: 487–498.
21. Gautam A, Kshirsagar AS, Banerjee S, et al. (2016) UVC-shielding by nano-TiO_2/PMMA composite: A chemical approach. *J Mater Sci Nanotechnol* 4: 304.
22. Bai Y, Li Z, Cheng B, et al. (2017) Higher UV-shielding ability and lower photocatalytic activity of TiO_2@SiO_2/APTES and its excellent performance in enhancing the photostability of poly(p-phenylene sulfide). *RSC Adv* 7: 21758–21767.
23. Liu S, Liu X, Latthe SS, et al. (2015) Self cleaning transparent superhydrophobic coatings through simple sol–gel processing of fluoroalkylsilane. *Appl Surf Sci* 351: 897–903.
24. Gobara M (2015) Effects of TiO_2/SiO_2 reinforced nanoparticles on the mechanical properties of green hybrid coatings. *Int Lett Chem Phys Astron* 47: 56–66.
25. Nadzirah S, Foo KL, Hashim U (2015) Moprhological reaction on the different stabilizers of titanium dioxide nanoparticles. *Int J Electrochem Sc* 10: 5498–5512.
26. Dong H, Lee M, Thomas RD, et al. (2003) Methyltrimethoxysilane sol–gel polymerization in acidic ethanol solutions studied by ^{29}Si NMR spectroscopy. *J Sol-Gel Sci Techn* 28: 5–14.
27. Lana SLB, Seddon AB (1998) X-Ray diffraction studies of sol–gel derived ORMOSILs based on combinations of tetramethoxysilane and trimethoxysilane. *J Sol-Gel Sci Techn* 13: 461–466.
28. Hakki A, Yang L, Wang F, et al. (2017) The effect of interfacial chemical bonding in TiO_2-SiO_2 composites on their photocatalytic NO_x abatement performance. *J Vis Exp* 125: 56070.
29. Wang Y, Li B, Liu T, et al. (2014) Controllable fabrication of superhydrophobic TiO_2 coating with improved transparency and thermostability. *Colloid Surface A* 441: 298–305.
30. Rubio F, Rubio J, Oteo JL (1998) A FT-IR study of the hydrolysis of tetraethylorthosilicate (TEOS). *Spectrosc Lett* 31: 199–219.
31. Tang Z, Hess DW, Breedveld V (2015) Fabrication of oleophobic paper with tunable hydrophilicity by treatment with non-fluorinated chemicals. *J Mater Chem A* 3: 14651–14660.
32. Socrates G (2001) *Infrared and Raman Characteristic Group Frequencie*s, Hoboken, USA: John Wiley & Sons Inc.
33. Bahşi ZB, Büyükaksoy A, Ölmezcan SM, et al. (2009) A novel label-free optical biosensor using synthetic oligonucleotides from *E. coli* O157:H7: elementary sensitivity tests. *Sensors* 9: 4890–4900.
34. Kunst SR, Beltrami LVR, Cardoso HRP, et al. (2015) Characterization of siloxane-poly(methyl methacrylate) hybrid films obtained on a tinplate substrate modified by the addition of organic and inorganic acids. *Mat Res* 18: 151–163.
35. Vasconcelos DCL, Costa VC, Nunes EHM, et al. (2011) Infrared spectroscopy of titania sol–gel coatings on 316L stainless steel. *Mater Sci Appl* 2: 1375–1382.
36. Boudot M, Ceratti DR, Faustini M, et al. (2014) Alcohol-assisted water condensation and stabilization into hydrophobic mesoporosity. *J Phys Chem C* 118: 23907–23917.
37. Latthe SS, Demirel AL (2013) Polystirene/octadecyltrichlorosilane superhydrophobic coatings with hierarchical morphology. *Polym Chem* 4: 246–249.

38. Lakshmi RV, Bera P, Anandan C, et al. (2014) Effect of the size of silica nanoparticles on wettability and surface chemistry of sol–gel superhydrophobic and oleophobic nanocomposite coatings. *Appl Surf Sci* 320: 780–786.
39. Mammer F, Le Bourhis E, Rozes L, et al. (2005) Mechanical properties of hybrid organic–inorganic materials. *J Mater Chem* 15: 3787–3811.
40. Li X, He J, Liu W (2013) Broadband anti-reflective and water repellent coatings on glass substrates for self-cleaning photovoltaic cells. *Mater Res Bull* 48: 2522–2528.